Towards a Molecular Understanding of the Detection of Amyloid Proteins With Flexible Conjugated Oligothiophenes.

ARTICLE *in* THE JOURNAL OF PHYSICAL CHEMISTRY A · SEPTEMBER 2014

Impact Factor: 2.69 · DOI: 10.1021/jp506797j · Source: PubMed

7 AUTHORS, INCLUDING:

Jonas Sjöqvist

6 PUBLICATIONS **19** CITATIONS

SEE PROFILE

Rozalyn A Simon

Linköping University

14 PUBLICATIONS **437** CITATIONS

SEE PROFILE

Mathieu Linares

Linköping University

63 PUBLICATIONS **978** CITATIONS

SEE PROFILE

Mikael Lindgren

Norwegian University of Science and Technol…

212 PUBLICATIONS **2,971** CITATIONS

SEE PROFILE

THE JOURNAL OF PHYSICAL CHEMISTRY A

Article

pubs.acs.org/JPCA

Toward a Molecular Understanding of the Detection of Amyloid Proteins with Flexible Conjugated Oligothiophenes

Jonas Sjöqvist,[†] Jerôme Maria,[‡] Rozalyn A. Simon,[†] Mathieu Linares,[†] Patrick Norman,*[,†] K. Peter R. Nilsson,[†] and Mikael Lindgren[‡,†]

[†]Department of Physics, Chemistry and Biology, Linköping University, SE-581 83 Linköping, Sweden

[‡]Department of Physics, Norwegian University of Science and Technology, NO-7491 Trondheim, Norway

Supporting Information

ABSTRACT: Molecular and electronic structures and optical absorption properties of oligothiophenes used for spectral assignment of amyloid deposits have been investigated for a family of probes known as luminescent conjugated oligothiophenes (LCOs). Theoretical absorption spectra have been determined using conformational averaging, combining classical molecular dynamics (MD) simulations with quantum mechanical/molecular mechanics (QM/MM) time-dependent density functional theory (TD-DFT) spectrum calculations. Theoretical absorption spectra are in excellent agreement with experiments, showing average errors below 5 nm for absorption maxima. To couple observed properties to molecular structures, a measure of planarity is defined, revealing a strong correlation between the transition wavelength of the first and dominating electronically excited state and dihedral rotations. It is shown that from this correlation, predictions can be made of the absorption properties of probes based only on information from MD trajectories. We show experimentally that red shifts observed in the excitation maxima of LCOs when bound to amyloid protein aggregates are also evident in absorption spectra. We predict that these red shifts are due to conformational restriction of the LCO in a protein binding pocket, causing a planarization of the conjugated backbone. On the basis of our studies of planarity, it is shown that such shifts are both possible and realistic.

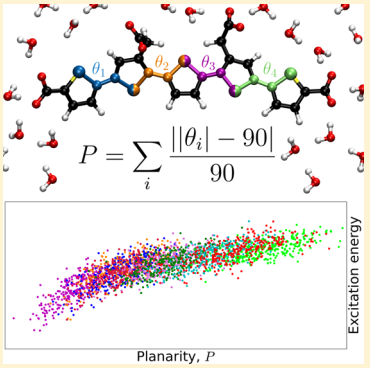

1. INTRODUCTION

Certain proteins and peptides misfold and self-associate in an abnormal manner into so-called amyloid deposits,[1] which are the pathological hallmarks of several diseases, such as Alzheimer's disease. The generic fibrillar structures have the ability to bind small molecules such as the widely used amyloid ligands thioflavin T (ThT) and Congo red.[2,3] This leads to alterations of optical and luminescent properties in terms of, for example, fluorescence quantum efficiency and polarization anisotropy, rendering the appearance of the ligands birefringent under crossed polarizers.[4] Recently, luminescent conjugated oligothiophenes (LCOs) have emerged as a novel class of ligands that can be utilized for studies of protein amyloid aggregates and related diseases.[5−7] In contrast to the traditional small hydrophobic fluorescent amyloid ligands, LCOs contain highly flexible conjugated thiophene backbones, the conformational state of which affects their spectroscopic properties.[8−12] Binding to protein aggregates is believed to constrain the rotational freedom of the thiophene backbones, altering their spectral properties in a conformation-sensitive manner. Thus, an optical fingerprint is obtained, unique to the structure of the protein. This property has been used to discriminate conformational heterogeneities in amyloid-β plaques in Alzheimer disease mouse models. In addition, LCOs have high multiphoton excitation capability, allowing in vivo studies of protein aggregation in animal disease models.[5]

Although the possibility of using the optical signatures of LCOs to make distinctions within heterogeneous populations of protein aggregates makes them a superior choice over other amyloid ligands, which only allow simple detection, an increased understanding of the correlation between specific spectroscopic signatures and distinct LCO conformations is still necessary to gain further insight into the morphology of disease-associated protein deposits. In this regard, we recently presented a theoretical model,[13] based on classical molecular mechanics (MM) and time-dependent density functional theory (TD-DFT), for assessing the effect of system dynamics on the luminescence properties of flexible conjugated chromophores. In this model, the dynamics of the system are simulated classically using a force field description with spectrum calculations performed on sampled structures using TD-DFT response theory, the average of which provides the final spectrum. Two model LCO compounds were investigated using this model, with absorption spectra calculated in a room-temperature water solution. For one of the LCO compounds, a fluorescence spectrum was also obtained based on excited-state molecular dynamics (MD) simulations. In addition, the dynamic behavior of the chromophores was studied in more detail, with structural properties tied to spectral properties. This

Received: July 8, 2014
Revised: September 19, 2014
Published: September 23, 2014

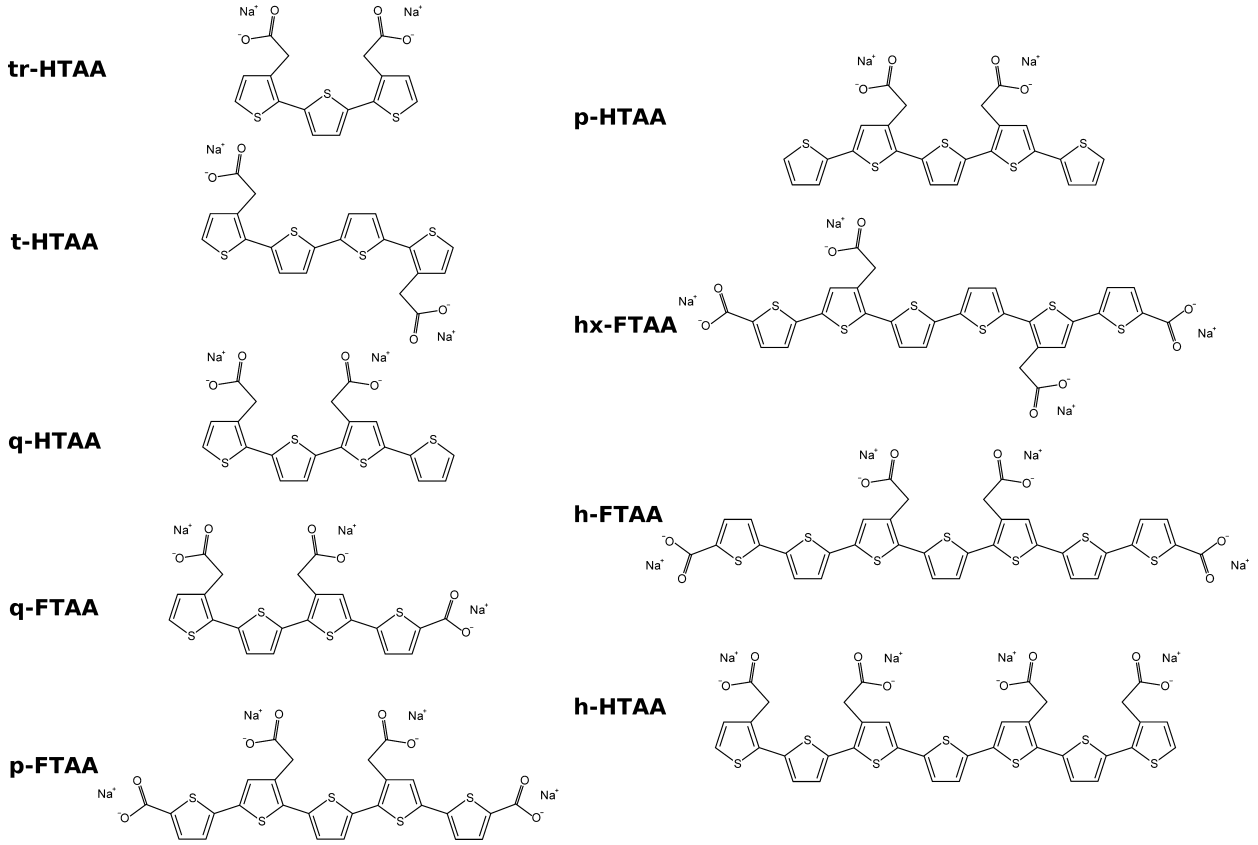

Figure 1. Molecular structures of the studied oligothiophene compounds.

method of conformational averaging was further extended with a solvent model for conjugated polyelectrolytes, with one of the LCOs used as an example.[14] A quantum mechanics/molecular mechanics (QM/MM) description was employed for an accurate inclusion of solvent effects in individual spectrum calculations.

In this work, we study a larger and more varied set of molecules,[6] both through optical spectroscopy measurements as well as the above-mentioned theoretical model. In addition to the two previously studied LCOs, p-HTAA and p-FTAA, we also include seven structurally related LCOs, varying the number of thiophene units and the carboxylate group positions. The results are analyzed with a focus on correlation between the excitation energy of the first electronically excited state and a measure of LCO planarity defined in this work. It is shown that this correlation can be used to make predictions regarding the spectral properties of other chromophores within the same family, based solely on information obtained from MD simulations. Using this, we further show that the calculated red shift of the absorption maximum upon planarization mimics that of the experimentally determined optical transition occurring when the oligothiophenes bind to insulin amyloid fibrils. This lends strength to the theory that the oligiothiophene backbone undergoes a planarization upon binding to amyloid fibrils, and we foresee that the results of these studies may form the basis for further theoretical calculations of oligothiophenes-based ligands interacting with protein aggregates.

2. METHODOLOGY

A. Conformational Averaging. As the rotational barriers between thiophene units in the LCOs are quite low,[15] the conventional approach of calculating absorption spectra by reference to zero temperature optimized structures is invalid. The low barriers allow the rings to rotate almost freely at room temperature, meaning that the LCOs are most often found in conformations distorted from the more planar optimized structures. As the UV/vis absorption spectra of the LCOs are dominated by $\pi-\pi^*$ transitions in the conjugated backbone, which are strongly connected to the planarity of the molecule, such distortions can have a major impact on the resulting spectrum. To take this consideration into account, this work uses a method of conformational averaging that follows that of our previous studies of flexible chromophores[13] as well as other similar works.[16,17] In this method, a MD simulation is run for the chromophore of interest in an appropriate environment and temperature, with use of a classical force field. From the simulation, a large number of uncorrelated structural snapshots are extracted, and a spectrum is calculated for each one of them using TD-DFT response theory. The final spectrum is then obtained as an average of all of the individual spectra.

The adopted method thus forgoes any explicit inclusion of vibrational states, relying instead on a representative sampling of the molecular structures from the MD simulations, with the following expression used to calculate the absorption from the ground state to the electronically excited state n

$$\sigma^{n\leftarrow 0}(\omega) \approx \frac{1}{N}\sum_{i=1}^{N} \Delta\omega_0^n(R_i)|\boldsymbol{\mu}(R_i)|^2 g[\omega - \Delta\omega_0^n(R_i)] \quad (1)$$

dx.doi.org/10.1021/jp506797j | J. Phys. Chem. A 2014, 118, 9820−9827

where the index i denotes samples taken from an MD trajectory and the coordinates R_i are the nuclear coordinates of that sample. The vertical electronic transition frequency of coordinates R_i are denoted by $\Delta\omega_0^n(R_i)$, and the electric transition dipole vector between states $|0\rangle$ and $|n\rangle$ is given by $\boldsymbol{\mu}(R_i)$. The function g is a line shape function that in a phenomenological way accounts for Franck−Condon broadening due to fast nuclear motions. The adopted scheme to treat only the slow nuclear motions in a rigorous manner is motivated by the fact that the predominant spectral broadening effects in the experiment are associated with the slow dihedral motions.

B. Solvation Models. The influence of the surrounding environment on the spectral properties of the chromophores can be divided into direct and indirect parts. The indirect part comes from the way that the environment affects the dynamics of the system, altering the conformational distribution of the solute. This is taken into account through the MD simulations, in which the full environment is included, and it is thus reflected in the structural sampling. The direct influence of the environment comes from the changes that it induces in the electronic charge distribution of the chromophore, as reflected in the spectrum calculations. This can be taken into account by partial inclusion of the solvent together with the solute in the QM system, but the computational price of such an expansion quickly makes the calculations highly demanding. For the conformational averaging method used in this work, where a large number of spectrum calculations are required, such an approach is not suitable, and for that reason, we have developed two more appropriate solvation models in a previous work.[14] The first of these uses the fact that the primary effect of the solvent is to screen the conjugated backbone of the LCO from its ionic side groups. On the basis of this, both the surrounding solvent as well as the carboxylate ions of the side groups are removed, with the carboxylate ions replaced by hydrogen atoms. This cut-down model is slightly less accurate but highly computationally efficient. The second model uses a QM/MM description of the system, with the solute described at the QM level and the solvent at the MM level, giving highly accurate results at a somewhat increased computational cost as compared to vacuum calculations.

3. EXPERIMENTAL DETAILS

The chemical structures of the studied set of LCOs are shown in Figure 1 along with their abbreviations. They were synthesized as previously described,[5,6] and absorbance measurements were performed by using a 1 cm quartz cell filled with 10 μM of the LCO in MQ water. A Shimamadzu UV-1601 PC UV−visible spectrophotometer was used for the absorption measurements. The spectral resolution of the excitation and emission monochromators was set to 5 nm.

A stock solution containing 320 μM bovine insulin in 25 mM HCl was prepared. The solution was placed in a water bath kept at 65 °C to induce amyloid formation. Samples were taken and analyzed after 24 h. First, q-FTAA, p-HTAA, and p-FTAA were dissolved in deionized water to a final concentration of 1.5 mM and then added either to deionized water or to 320 μM bovine insulin amyloid fibrils (in 10 mM HCl) to a final concentration of 10 μM. After 10 min of incubation, absorption spectra were collected between 350 and 550 nm, using a Tecan Saphire 2 plate reader (Tecan Group Ltd., Mannedorf, Switzerland).

4. COMPUTATIONAL DETAILS

All MD simulations were performed using the CHARMM force field[18] as implemented in the Tinker program.[19] The parameters used were taken from the CHARMM22 set,[20] with the exception of those reparameterized in our previous work.[13,14] The atomic charges used were taken from the PCFF force field.[21,22] All MD simulations were carried out in the canonical ensemble at a temperature of 300 K and using the Berendsen thermostat[23] with an integration step of 1 fs.

Each LCO was solvated by placing it in a box filled with thermally equilibrated water molecules at a concentration of 1.0 g/cm^{-3}, removing any overlapping water molecules. Due to the varying sizes of the studied LCOs, boxes of different sizes were used, with a square box with the side 34.1 Å used for all LCOs with a length of five thiophene units or less and larger rectangular boxes used for the longer LCOs. Table 1 summarizes the sizes of the boxes used as well as the number of water molecules contained in them, with small variations due to the different sizes of the LCOs. For all simulations, an initial equilibration of 100 ps was run, after which six snapshots were collected at 20 ps intervals. These snapshots were then used as starting points for six separate MD simulations of 500 ps. From each of these simulations in turn, 50 snapshots were collected, with sampling starting after 100 ps and at 8 ps intervals. This produced a total of 300 structural snapshots for each chromophore.

Table 1. Dimension of the Boxes Used in the MD Simulations, with Lengths Given in Å, as Well as the Number of Water Molecules Contained in the Boxes

LCO	x	y	z	number of water molecules
tri- to pentamers	34.1	34.1	34.1	1304−1313
hx-HTAA	40.3	34.1	34.1	1552
hx-FTAA	43.4	40.3	40.3	2339
h-HTAA, h-FTAA	46.5	43.4	43.4	2903, 2904

All absorption spectrum calculations were carried out with the Dalton program[24,25] at the TD-DFT level of theory and using the Coulomb attenuated B3LYP (CAM-B3LYP)[26] exchange−correlation functional in conjunction with the aug-cc-pVDZ basis set. The individual spectrum calculations were carried out using a cut-down model, in which the solvent is completely neglected and each carboxylate group is replaced by a hydrogen atom. High-quality comparison calculations were performed using a QM/MM model in which a QM description is employed for the solute while the surrounding solvent uses the polarizable MM potential of Ahlström and co-workers.[27] The model used includes a 5 Å layer of polarizable water around the solute, surrounded by a further 10 Å of nonpolarizable water.[14] For the line shape function in eq 1, a unit amplitude Gaussian was used with a half-width, half-maximum line broadening of 0.1 eV, which corresponds to 13 nm in the region around 400 nm.

Geometry optimizations were performed using the Gaussian 09 program,[28] employing the B3LYP functional together with the cc-pVTZ basis set. The optimizations were carried out for each LCO in the all-trans conformation, using the cut-down model and with planarity enforced between the thiophene rings.

dx.doi.org/10.1021/jp506797j | J. Phys. Chem. A 2014, 118, 9820−9827

5. RESULTS

A. Optical Characterization of LCOs. Averaged room-temperature absorption spectra were calculated for all LCOs using the computationally efficient cut-down model, as detailed in section 2B. The choice of this approximate model was made due to the large number of spectra needed as well as the large sizes of the systems, thereby requiring significant computational resources even with the efficient cut-down model. To gauge the quality of the obtained spectra, a small number of higher-accuracy calculations were performed for each chromophore. In these, the high-quality QM/MM model, also described in section 2B, was employed, with spectra calculated for 12 snapshots for each of the chromophores, taken from the selection made for the full averaged spectrum. Each QM/MM calculation was compared to the equivalent calculation performed using the cut-down model in order to find the shift of the dominant excited state, ΔE, as well as the factor by which the oscillator strengths change, S_f. The shifts and factors for all LCOs, as well as their standard deviations, σE and σS_f, can be found in Table 2. As the small values of the standard deviations show, the errors made in employing the cut-down model are quite systematic, and results can thus be corrected by means of energy shifts and scaling of oscillator strengths. All plotted spectra in this work have had this QM/MM correction applied, with the corrected and uncorrected transition wavelengths of the main peaks reported in Table 3. In addition to the calculated transition wavelengths, theoretical estimates of the extinction coefficients for the LCOs are also available in the table, obtained from numerical integration over the averaged spectrum and normalized to the experimental value found for q-HTAA. These estimates are given both with and without the QM/MM correction applied.

Table 2. Average Excitation Shifts and Oscillator Strength Scaling Factors for the LCOs When Going from the Cut-down to the QM/MM Model, with Standard Deviations

LCO	ΔE (eV)	σE (eV)	S_f	σS_f
tr-HTAA	−0.061	0.033	1.09	0.03
t-HTAA	−0.061	0.028	1.08	0.03
q-HTAA	−0.065	0.035	1.05	0.03
q-FTAA	−0.132	0.035	1.22	0.04
p-HTAA	−0.064	0.046	1.01	0.05
p-FTAA	−0.166	0.081	1.17	0.09
hx-FTAA	−0.107	0.022	1.19	0.03
h-FTAA	−0.082	0.035	1.17	0.09
h-HTAA	−0.033	0.018	1.03	0.02

Table 3. Experimental and Theoretical Absorption Maxima and Extinction Coefficients for the LCOs[a]

	absorption maximum (nm)			extinction coefficient (cm^{-1} mol^{-1})		
LCO	expt.	cut-down	QM/MM	expt.	cut-down	QM/MM
tr-HTAA	338	345	351	16000	19500	20300
t-HTAA	378	380	387	29000	26200	27000
q-HTAA	371	371	378	26900	26900	26900
q-FTAA	385	364	379	23000	26800	31200
p-HTAA	394	383	391	35000	34900	33600
p-FTAA	409	388	409	48000	35000	39000
hx-FTAA	428	419	434	52000	43700	49600
h-FTAA	434	421	432	55000	53000	59000
h-HTAA	430	428	433	48000	50800	49800

[a]Theoretical results are reported both with and without the QM/MM correction.

In Figure 2, experimental and theoretical optical absorption spectra are shown for chromophores of varying chain length, from trimer to heptamer. From this sample of spectra, we note a clear trend of increasing extinction coefficient and a red shift of the optical absorption as the molecular length increases and, thereby, the π-conjugated network becomes more extended. These trends are well described in the theoretical calculations, but, as is evident from the theoretical extinction coefficients found in Table 3, the relative absorption strengths of the LCOs have not been fully captured by the theoretical model. The QM/MM correction improves the results, and the general trend of increasing absorption strength for increasing molecule size is found, but more subtle differences between molecules are not reliably replicated.

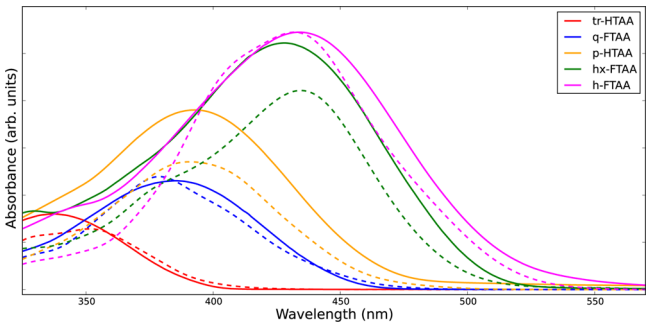

Figure 2. Experimental (solid) and theoretical (dashed) absorption spectra. The theoretical spectra have been normalized so that the strengths of the experimental and theoretical peaks of h-FTAA agree.

The theoretical spectral profiles are in excellent agreement with experiment, even capturing the inhomogeneous broadenings when such occur. This is more clearly seen in the individual spectra, as supplied in the Supporting Information, and indicates that the spectral broadenings are predominantly due to dihedral rotations as described by the method of conformational averaging.

In Table 3, absorption maxima are reported for the complete set of LCOs. The calculated transition wavelengths are, without exceptions, in very good agreement with those extracted from the measurements, with differences in experimental and theoretical absorption maxima varying from 13 nm for tr-HTAA to 0 for p-FTAA. The average error is 5 nm, showing excellent agreement for the set as a whole. The absorption maxima are also shown in Figure 3, visualizing the correlation between theoretical and experimental values, both before and after the QM/MM corrections have been applied. This shows that the correction is most important for the F variants, for which there are carboxylate groups on the terminating thiophene rings, extending the conjugated system. Removal of these groups in the cut-down model causes a significant blue shift of the absorption spectrum, which is accounted for in the QM/MM correction, causing a much improved agreement with experiments.

B. Structural Properties. The LCO absorption spectra are dominated by the first electronically excited state to such a degree that the main peak of the averaged spectra exists

dx.doi.org/10.1021/jp506797j | J. Phys. Chem. A 2014, 118, 9820−9827

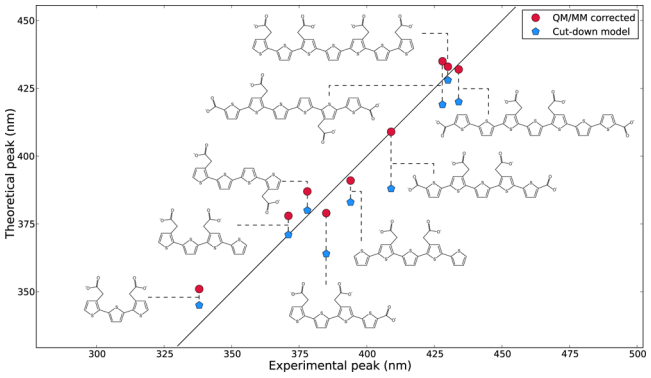

Figure 3. Correlation between experimental and theoretical peaks for the LCOs, with theoretical peaks shown both before and after the QM/MM correction has been applied. The straight line indicates perfect agreement between theory and experiment.

exclusively due to this excitation. Because the excitation in question is a $\pi \rightarrow \pi^*$ transition, it is strongly connected to the planarity of the molecule, becoming increasingly blue shifted as the thiophene rings are twisted out of plane, breaking the conjugated system. On the basis of this knowledge, a measure of planarity, P, can be defined as

$$P = \sum_i \frac{||\theta_i| - 90|}{90} \tag{2}$$

where θ_i is the dihedral angle formed between two adjacent thiophene rings, defined between −180 and 180°, and where the sum ranges over all such angles in the chromophore. Thus, for each bond between two thiophene rings, a value between 0 and 1 is added to the sum, where 0 indicates that the two rings are completely out of plane with each other and 1 indicates that the are completely planar. This definition has the advantage of allowing comparisons between LCOs of different length as all LCOs have a common minimum in $P = 0$, where every thiophene ring is completely out of plane with its neighbors, indicating a completely broken conjugated system but with different maxima depending on the length of the system. Longer chromophores, capable of containing longer conjugated systems, thus have the possibility of a higher measure of planarity, with an LCO containing n thiophene units having a maximum value of $P = n - 1$.

For each LCO, P was calculated for all 300 structural snapshots used in the calculation of the averaged spectrum and was then checked for a correlation with the excitation energy of the first electronically excited state of the corresponding spectrum calculation. A strong correlation was found between the structure and excitation wavelength of each chromophore, with correlation coefficients varying from −0.80 for the shortest LCO, tr-HTAA, to −0.69 for the longest, h-FTAA, with a correlation coefficient of −0.81 found for the total set. The top panel of Figure 4 shows a scatter plot illustrating this correlation.

As the measure P incorporates not just the geometry of the molecule but also its length, with the maximum P varying with the number of thiophene units in the LCO, it is of interest to see how these two contributions can be separated. First, the length dependence was investigated by calculating the absorption spectra for geometry-optimized structures in which the thiophene rings are kept fully planar, that is, with a maximum P. This was done for the cut-down model, with the

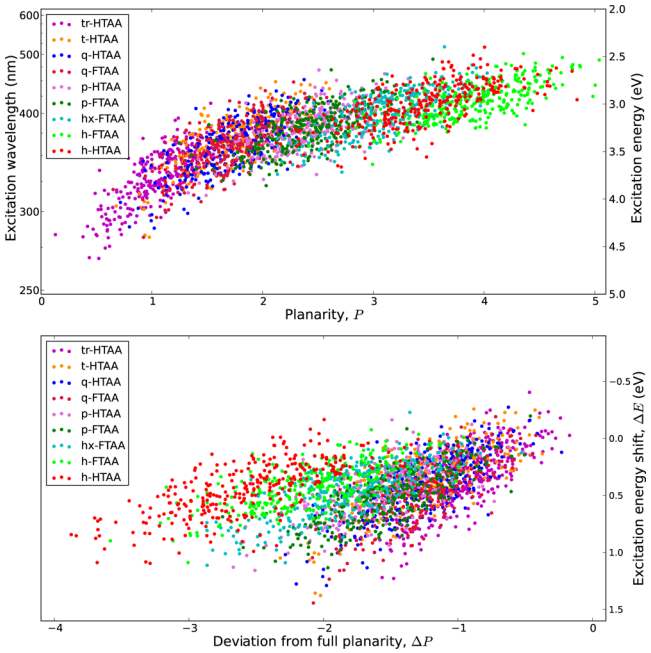

Figure 4. (Top panel) Correlation between LCO planarity, P, defined in eq 2, and the excitation energy of the first electronically excited state. Each molecule is represented by 300 points, corresponding to the snapshots used for the averaged spectra. (Bottom panel) Correlation between the deviation from full planarity, ΔP, and the shift in the first electronically excited state as compared to that of the fully planar LCO, ΔE.

QM/MM correction applied afterward. The resulting absorption maxima are shown in Table 4, which also includes the

Table 4. Theoretical Absorption Maxima, Given in eV and with the QM/MM Correction Applied, of the LCOs for the Average Spectra, E_{avg}, and for Ideal, Planar Geometries, E_{planar}[a]

LCO	E_{avg}	E_{planar}	ΔE	P_{avg}	P_{planar}	ΔP
tr-HTAA	3.53	3.40	0.13	1.08	2.00	−0.92
t-HTAA	3.20	3.02	0.18	1.77	3.00	−1.23
q-HTAA	3.28	3.02	0.26	1.75	3.00	−1.25
q-FTAA	3.27	2.96	0.31	1.73	3.00	−1.27
p-HTAA	3.17	2.81	0.36	2.44	4.00	−1.56
p-FTAA	3.03	2.72	0.31	2.46	4.00	−1.54
hx-FTAA	2.86	2.63	0.23	3.18	5.00	−1.82
h-FTAA	2.87	2.55	0.32	3.90	6.00	−2.10
h-HTAA	2.86	2.57	0.29	3.45	6.00	−2.55

[a] P_{avg} is the average planarity for the sampled structures, and P_{planar} is the planarity of the flat geometry. ΔE and ΔP show the deviation from this geometry for absorption maxima and planarity, respectively.

absorption maxima of the averaged spectra as well as the average and maximum P value for each LCO. In addition, the deviation from the planar geometry is reported, both for the absorption maximum, ΔE, and the planarity, ΔP. As can be expected, the absorption spectra become more red shifted as the length of the LCOs increases, with additional thiophene units causing larger shifts and the extra carboxylate ions of the F variants causing smaller shifts. To isolate the geometrical aspect of the planarity measurement, the correlation between ΔP and ΔE was investigated for the structural snapshots of each LCO, with the resulting scatter plot shown in the lower panel of

dx.doi.org/10.1021/jp506797j | J. Phys. Chem. A 2014, 118, 9820−9827

Figure 4. In this figure, it is of interest to note that there exists a small number of snapshots that result in a red shift of the excitation energy as compared to that of the planar geometry, showing that structural properties other than the planarity are also capable of influencing the spectrum.

While this parameter of planarity does not reflect all aspects of the molecular structure, lacking both the distinction between many small disturbances to the planarity spread over a molecule and a single large disturbance in one location as well as any sort of weighting based on the position of the disturbance, it is still a valuable tool that allows insight into the spectrum of a LCO solely from a simple analysis of the MD trajectory. It allows comparisons to be made between different chromophores or between the same chromophore in different environments, where relative shifts and changes in width of the distribution of P are likely to be mirrored in the absorption spectrum. The large differences between chromophores of different length can be clearly seen, even in the scatter plot of Figure 4, but the planarity measure is also capable of capturing more subtle effects, such as the difference between the two tetramers t-HTAA and q-HTAA. The only difference in structure between the two lies in the placement of one of the substituent arms, with the distance between the arms being two thiophene units for t-HTAA and one for q-HTAA. The repulsion between the ionic groups can be expected to cause q-HTAA to be less planar than t-HTAA, resulting in a more broken conjugated system and a blue-shifted spectrum. The experimental and calculated spectra confirm this, showing the main peak of q-HTAA as blue shifted by 7 and 9 nm compared to t-HTAA, respectively. However, it is also possible to predict the shift based on the planarity as the average P found for the sampled structures of q-HTAA is 1.75, indicating a slight blue shift compared to the average P found for t-HTAA, 1.77.

In addition, it is possible to use the distribution of P to ensure that the sampling used for an averaged spectrum calculation is accurate. A sampling needs to fulfill two requirement to properly represent the conformational distribution of the chromophore. First, it must come from a MD trajectory that is long enough that the chromophore has been allowed to fully explore the conformational space, and second, the number of samples must be high enough that all aspects of that space can be represented. Both of these issues can be addressed with the use of P, the first by making sure that the distribution of P is converged when increasing the length of the trajectory and the second by ensuring that the planarity distribution for the sampled structures is the same as that for the trajectory as a whole.

C. Spectral Shifts in Absorption upon Binding to Insulin Fibrils. Previous studies have shown that upon binding to protein aggregates, LCOs exhibit decreased Stokes shifts, with red-shifted excitation maxima and blue-shifted emission maxima compared to free dyes in solution.[5−7] To see if the same shifts are displayed also in the absorption spectra of the LCOs, three oligothiophenes in terms of q-FTAA, p-HTAA, and p-FTAA were tested toward insulin amyloid fibrils. Figure 5 shows absorption spectra for the three chromophores, both in deionized water and mixed with insulin amyloid fibrils. Red shifts are observed in all cases going from water to protein, with absorption maxima in water found at 385, 394, and 409 nm and those with protein at 425, 434, and 427 nm for q-FTAA, p-HTAA, and p-FTAA, respectively. Hence, these LCOs give drastically distinct and different optical responses when bound to protein aggregates such as insulin amyloid fibrils. Similar

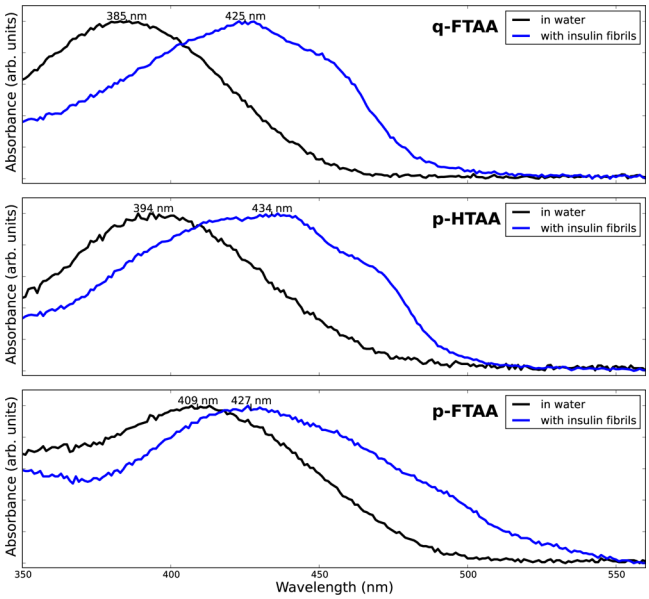

Figure 5. Absorption spectra of q-FTAA, p-HTAA, and p-FTAA in deionized water or bound to insulin amyloid fibrils.

observations have been reported also for other amyloid types, such as amyloid-β plaques and prion deposits.[5−7] Such spectral changes are usually monitored from the excitation spectrum obtained from the fluorescence emission signal, but we have now shown that such spectral shifts are also associated with a distinct shift of the optical absorption. Thus, the previously described theoretical calculations of absorption spectra, as well as their correlation to the planarity of the backbone, can also be used to gain an understanding of the LCO conformations when bound to amyloid fibrils.

The proposed explanation for the observed shifts is that the dihedral rotations of the conjugated backbone of the LCOs become constrained when bound to an amyloid protein. The more planar structures in the protein environment as compared to those in the liquid phase lead to red shifts in absorption spectra. Furthermore, it has been shown that the excited-state configuration becomes fully planar as a consequence of photoexcitation,[13] a structure relaxation that, if partly hindered by the protein, will lead to blue shifts in fluorescence spectra. The plausibility of such an explanation has been investigated based on the measure of planarity discussed in section 5B and its strong correlation to the excitation energies of the LCOs. The measured red shifts observed for q-FTAA, p-HTAA, and p-FTAA when going from water to the protein environment are 0.30, 0.29, and 0.11 eV, respectively. On the basis of a least-squares fit to the sampled data seen in Figure 4, the approximate linear dependence of the excitation energy to the planarity was found for each of the three chromophores. Using this, the changes in planarity required to produce red shifts equivalent to those found experimentally were extrapolated. The shifts were then applied to the average planarity found for the sampled data, with the results summarized in Table 5. For all three LCOs, the required increase in planarity is well within realistic limits, corresponding to an average distortion from full planarity of 22, 20, and 29° per dihedral angle for q-FTAA, p-HTAA, and p-FTAA, respectively. Keeping the average planarity around these values could very well be achieved in a restricting pocket of the protein aggregate. As such, conformational restriction appears a likely explanation

dx.doi.org/10.1021/jp506797j | J. Phys. Chem. A 2014, 118, 9820−9827

Table 5. Experimental Absorption Maxima of LCOs with Water and with Amyloid Proteins, in eV[a]

LCO	E_{water}	$E_{protein}$	ΔE	P_{avg}	P_{fit}	P_{max}
q-FTAA	3.22	2.92	−0.30	1.73	2.27	3.00
p-HTAA	3.15	2.86	−0.29	2.44	3.09	4.00
p-FTAA	3.03	2.92	−0.11	2.46	2.73	4.00

[a] P_{avg} is the average planarity found in water, P_{fit} is the fitted planarity, which corresponds to an applied shift of ΔE, and P_{max} is the maximum planarity of the molecule.

for the observed spectral shifts, with the next logical step in this study being simulations of LCOs together with protein fibril models. By comparing the LCO planarity distributions in different binding pockets in the protein aggregate, it will be possible to more firmly deduce whether they are capable of producing the expected spectral shifts. In addition, the change from a water to protein environment can have a small influence on the spectral properties, something that would be revealed in such a study. To construct a realistic model of these fibrillar bundles is, however, currently hampered by the lack of crystalline structure data as well as computational constraints with regard to system sizes.

6. CONCLUSIONS

Absorption spectra have been obtained for a series of nine oligothiophenes used in amyloid fibril characterization, both through experimental and theoretical means. The theoretical calculations were performed using a previously developed model, combining classical MD simulations with QM/MM TD-DFT spectrum calculations. The resulting theoretical spectra are in excellent agreement with experiments, both with regard to the position of the absorption maxima, showing an average error of just 5 nm, as well as the shape of the spectral profiles.

On the basis of the theoretical calculations, we have defined a structural property of planarity, showing a strong correlation to the first electronically excited state of the LCOs, which dominates the UV/vis spectra. Statistics for this planarity measurement can be extracted from MD trajectories, allowing computationally efficient predictions of spectral properties to be made, not just for the studied set of LCOs but for structurally related molecules as well.

We have shown experimentally that the red shifts exhibited in the excitation maxima of the LCOs when bound to amyloid fibrils are also evident in the absorption spectra. Using the measure of planarity, we have demonstrated that these spectral shifts can be replicated through a planarization of the conjugated backbone, and from this we predict that the LCOs are bound to the protein in a conformationally restricting pocket.

■ ASSOCIATED CONTENT

Supporting Information

Separate experimental and theoretical absorption spectra for each studied luminescent conjugated oligothiophene are provided. This material is available free of charge via the Internet at http://pubs.acs.org.

■ AUTHOR INFORMATION

Corresponding Author

*E-mail: panor@ifm.liu.se. Phone: +46-13281688.

Notes

The authors declare no competing financial interest.

■ ACKNOWLEDGMENTS

We acknowledge financial support from the Swedish Research Council (Grant No. 621-2010-5014) as well as a grant for computing time at the National Supercomputer Centre (NSC), Sweden. M.L. thanks the Swedish e-Science Research Center (SeRC) for financial support. Our work is supported by the Swedish Foundation for Strategic Research (K.P.R.N., R.A.S.). K.P.R.N. is financed by an ERC Starting Independent Researcher Grant (Project: MUMID) from the European Research Council. R.A.S. is enrolled in the doctoral program Forum Scientum. M.L. is grateful to Linköping University for a guest professorship. Parts of this work were supported by the LUPAS project supported by the EU FP7 program.

■ REFERENCES

(1) Chiti, F.; Dobson, C. M. Protein Misfolding, Functional Amyloid, and Human Disease. *Annu. Rev. Biochem.* **2006**, *75*, 333−366.

(2) Naiki, H.; Higuchi, K.; Hosokawa, M.; Takeda, T. Fluorometric Determination of Amyloid Fibrils *in Vitro* Using the Fluorescent Dye, Thioflavin T1. *Anal. Biochem.* **1989**, *177*, 244−249.

(3) Klunk, W. E.; Pettegrew, J. W.; Abraham, D. J. Quantitative Evaluation of Congo Red Binding to Amyloid-Like Proteins with a Beta-Pleated Sheet Conformation. *J. Histochem. Cytochem.* **1989**, *37*, 1273−1281.

(4) Lindgren, M.; Hammarström, P. Amyloid Oligomers: Spectroscopic Characterization of Amyloidogenic Protein States. *FEBS J.* **2010**, *277*, 1380−1388.

(5) Åslund, A.; Sigurdson, C. J.; Klingstedt, T.; Grathwohl, S.; Bolmont, T.; Dickstein, D. L.; Glimsdal, E.; Prokop, S.; Lindgren, M.; Konradsson, P.; et al. Novel Pentameric Thiophene Derivatives for *in Vitro* and *in Vivo* Optical Imaging of a Plethora of Protein Aggregates in Cerebral Amyloidoses. *ACS Chem. Biol.* **2009**, *4*, 673−684.

(6) Klingstedt, T.; Åslund, A.; Simon, R. A.; Johansson, L. B. G.; Mason, J. J.; Nyström, S.; Hammarström, P.; Nilsson, K. P. R. Synthesis of a Library of Oligothiophenes and Their Utilization as Fluorescent Ligands for Spectral Assignment of Protein Aggregates. *Org. Biomol. Chem.* **2011**, *9*, 8356−8370.

(7) Klingstedt, T.; Shirani, H.; Åslund, K. O. A.; Cairns, N. J.; Sigurdson, C. J.; Goedert, M.; Nilsson, K. P. R. The Structural Basis for Optimal Performance of Oligothiophene-Based Fluorescent Amyloid Ligands: Conformational Flexibility Is Essential for Spectral Assignment of a Diversity of Protein Aggregates. *Chem.—Eur. J.* **2013**, *19*, 10179−10192.

(8) Roux, C.; Leclerc, M. Rod-to-Coil Transition in Alkoxy-Substituted Polythiophenes. *Macromolecules* **1992**, *25*, 2141−2144.

(9) Faïed, K.; Fréchette, M.; Ranger, M.; Mazerolle, L.; Lévesque, I.; Leclerc, M.; Chen, T.; Rieke, R. D. Chromic Phenomena in Regioregular and Nonregioregular Polythiophene Derivatives. *Chem. Mater.* **1995**, *7*, 1390−1396.

(10) Leclerc, M.; Faid, K. Electrical and Optical Properties of Processable Polythiophene Derivatives: Structure−Property Relationships. *Adv. Mater.* **1997**, *9*, 1087−1094.

(11) Garreau, S.; Leclerc, M.; Errien, N.; Louarn, G. Planar-to-Nonplanar Conformational Transition in Thermochromic Polythiophenes: A Spectroscopic Study. *Macromolecules* **2003**, *36*, 692−697.

(12) Psonka-Antonczyk, K. M.; Duboisset, J.; Stokke, B. T.; Zako, T.; Kobayashi, T.; Maeda, M.; Nyström, S.; Mason, J.; Hammarström, P.; Nilsson, K. P. R.; et al. Nanoscopic and Photonic Ultrastructural Characterization of Two Distinct Insulin Amyloid States. *Int. J. Mol. Sci.* **2012**, *13*, 1461−1480.

(13) Sjöqvist, J.; Linares, M.; Lindgren, M.; Norman, P. Molecular Dynamics Effects on Luminescence Properties of Oligothiophene Derivatives: A Molecular Mechanics−Response Theory Study Based on the CHARMM Force Field and Density Functional Theory. *Phys. Chem. Chem. Phys.* **2011**, *13*, 17532−17542.

(14) Sjöqvist, J.; Linares, M.; Mikkelsen, K. V.; Norman, P. QM/MM-MD Simulations of Conjugated Polyelectrolytes: A Study of

Luminescent Conjugated Oligothiophenes for Use as Biophysical Probes. *J. Phys. Chem. A* **2014**, *118*, 3419−3428.
(15) González Cano, R. C.; Herrera, H.; Seguera, J. L.; López Navarrete, J. T.; Ruiz Delgado, M. C.; Casado, J. Conformational Control of the Electronic Properties of an $\alpha-\beta$ Terthiophene: Lessons from a Precursor Towards Dendritic Hyperbranched Oligo- and Polythiophenes. *ChemPhysChem* **2012**, *13*, 3893−3900.
(16) Kongsted, J.; Osted, A.; Mikkelsen, K. V.; Christiansen, O. The QM/MM Approach for Wavefunctions, Energies and Response Functions within Self-Consistent Field and Coupled Cluster Theories. *Mol. Phys.* **2002**, *100*, 1813−1828.
(17) Nielsen, C. B.; Christiansen, O.; Mikkelsen, K. V.; Kongsted, J. Density Functional Self-Consistent Quantum Mechanics/Molecular Mechanics Theory for Linear and Nonlinear Molecular Properties: Applications to Solvated Water and Formaldehyde. *J. Chem. Phys.* **2007**, *126*, 154112−154300.
(18) Brooks, B. R.; Bruccoleri, R. E.; Olafson, B. D.; States, D. J.; Swaminathan, S.; Karplus, M. CHARMM—A Program for Macromolecular Energy, Minimization, and Dynamics Calculations. *J. Comput. Chem.* **1983**, *4*, 187−217.
(19) Ponder, J. W. *TINKER*, version 5.0. Washington University: St. Louis, MO, 2009.
(20) MacKerell, A. D., Jr.; Bashford, D.; Bellott, M.; Dunbrack, R. L., Jr.; Evanseck, J. D.; Field, M. J.; Fischer, S.; Gao, J.; Guo, H.; Ha, S.; et al. All-Atom Empirical Potential for Molecular Modeling and Dynamic Studies of Proteins. *J. Phys. Chem. B* **1998**, *102*, 3586.
(21) Maple, J. R.; Dinur, U.; Hagler, A. T. Derivation of Force Fields for Molecular Mechanics and Dynamics from *Ab Initio* Energy Surfaces. *Proc. Natl. Acad. Sci. U. S. A.* **1988**, *85*, 5350−5354.
(22) Maple, J. R.; Hwang, M. J.; Stockfisch, T. P.; Dinur, U.; Waldman, M.; Ewig, C. S.; Hagler, A. T. Derivation of Class II Force Fields. I. Methodology and Quantum Force Field for the Alkyl Functional Group and Alkane Molecules. *J. Comput. Chem.* **1994**, *15*, 162−182.
(23) Berendsen, H. J. C.; Postma, J. P. M.; van Gunsteren, W. F.; DiNola, A.; Haak, J. R. Molecular Dynamics with Coupling to an External Bath. *J. Chem. Phys.* **1984**, *81*, 3684−3690.
(24) *DALTON*, a molecular electronic structure program, release DALTON2013.0. http://daltonprogram.org (2013).
(25) Aidas, K.; Angeli, C.; Bak, K. L.; Bakken, V.; Bast, R.; Boman, L.; Christiansen, O.; Cimiraglia, R.; Coriani, S.; Dahle, P.; et al. The Dalton Quantum Chemistry Program System. *WIREs Comput. Mol. Sci.* **2014**, *4*, 269−284.
(26) Yanai, T.; Tew, D. P.; Handy, N. C. A New Hybrid Exchange−Correlation Functional Using the Coulomb-Attenuating Method (CAM-B3LYP). *Chem. Phys. Lett.* **2004**, *393*, 51−57.
(27) Ahlström, P.; Wallqvist, A.; Engström, S.; Jönsson, B. A Molecular Dynamics Study of Polarizable Water. *Mol. Phys.* **1989**, *68*, 563−581.
(28) Frisch, M. J.; Trucks, G. W.; Schlegel, H. B.; Scuseria, G. E.; Robb, M. A.; Cheeseman, J. R.; Scalmani, G.; Barone, V.; Mennucci, B.; Petersson, G. A.; et al. *Gaussian 09*, revision A.02; Gaussian, Inc.: Wallingford, CT, 2004.